Computers in Biology and Medicine 113 (2019) 103423

Contents lists available at ScienceDirect

Computers in Biology and Medicine

journal homepage: http://www.elsevier.com/locate/compbiomed

Gabor wavelet-based deep learning for skin lesion classification

Sertan Serte [a,*], Hasan Demirel [b,**]

[a] Electrical and Electronic Engineering, Near East University, Nicosia, North Cyprus via Mersin 10, Turkey
[b] Electrical and Electronic Engineering, Eastern Mediterranean University, Famagusta, North Cyprus via Mersin 10, Turkey

ARTICLE INFO

Keywords:
Convolutional neural networks
Gabor wavelets
Model fusion

ABSTRACT

Skin cancer cases are increasing and becoming one of the main problems worldwide. Skin cancer is known as a malignant type of skin lesion, and early detection and treatment are necessary. Malignant melanoma and seborrheic keratosis are known as common skin lesion types. A fast and accurate medical diagnosis of these lesions is crucial. In this study, a novel Gabor wavelet-based deep convolutional neural network is proposed for the detection of malignant melanoma and seborrheic keratosis. The proposed method is based on the decomposition of input images into seven directional sub-bands. Seven sub-band images and the input image are used as inputs to eight parallel CNNs to generate eight probabilistic predictions. Decision fusion based on the sum rule is utilized to classify the skin lesion. Gabor based approach provides directional decomposition where each sub-band gives isolated decisions that can be fused for improved overall performance. The results show that the proposed method outperforms alternative methods in the literature developed for skin cancer detection.

1. Introduction

Cancer is one of the main problems worldwide [1]. The disease can take in several forms and occurs in different locations of the human body. One of the most commonly seen and deadly cancer types in women is breast cancer. Another widely recognized and cancer type with high mortality rates among men is prostate cancer. Melanoma skin cancer is also common and deadly among men and women. This type of cancer is known as the most commonly treated skin cancer type, and 9% of the population is affected in the United States. Moreover, it has also been reported that melanoma skin cancer type is the leading cause of cancer-related deaths in the United States. A recent study [1] has reported the estimated number of new cases and new cancer-related deaths.

Melanoma is one of the skin cancer types, and its associated mortality rate is higher than other types of skin cancer. This malignant type also causes more deaths than different skin cancer types, [2–4]. Melanoma and nevus are known as melanocytic skin lesions. Non-melanocytic skin lesions also occur in malignant and benign forms. Basal cell and squamous cell carcinoma are non-melanocytic malignant skin lesions. Actinic keratosis is the early form of squamous cell carcinoma. Dermatofibroma, vascular, and benign keratosis are known as non-melanocytic benign lesions. Although Basal-cell and squamous-cell carcinoma are more common, melanoma causes a greater number of deaths, [2,5].

Early detection of skin cancer leads to effective treatment. Early detection of cancer could be achieved via automated detection of cancer types using deep learning techniques. Recent studies show that accurate automatic detection of skin cancer can be achieved using deep convolutional neural networks (CNNs). Recent surveys [6–8] have also explained the automated detection of skin cancer forms.

Esteva et al. [1]. used a single GoogleNet CNN model [9,10] for skin lesion prediction. Han et al. [2]. also utilized the ResNet-152 CNN model [11] for skin cancer type recognition. Kaymak and Serener [12] used several single CNN models for the prediction of different categories of skin lesions. On the other hand, several studies have used an ensemble of CNN models for skin cancer detection. Hagari [13] combined AlexNet [14], GoogleNet, VGG [15], RestNet for lesion prediction. Mahbod [16] proposed to fusion of AlexNet, ResNet-18, ResNet-100 and VGG16 for malignant type lesion classification.

The proposed method is different than the above mentioned methods. The proposed new model contains several Gabor wavelet and skin image-based CNN models. This method is an extension of previous techniques and utilizes Gabor representations in a unified CNN model.

* Corresponding author.
** Corresponding author.
E-mail address: sertan.serte@neu.edu.tr (S. Serte).
URL: http://www.neu.edu.tr (S. Serte).

https://doi.org/10.1016/j.compbiomed.2019.103423
Received 29 June 2019; Received in revised form 9 August 2019; Accepted 29 August 2019
Available online 4 September 2019

The model also allows the integration of image data for further enhancements. The Gabor wavelet-based deep convolutional neural network method utilizes Gabor filters on skin images to obtain detailed representations of the skin lesions. Then these details are modeled using deep convolutional neural network models. Furthermore, the fusion of skin images and Gabor representations is performed to increase the accuracy of the proposed method. All details are modeled using deep networks, and then outputs are fused using a probabilistic fusion method to detect skin cancer types.

Previous studies [12,13,16,21] have used skin images as inputs and an ensemble of CNN models for the prediction of skin lesion types. In contrast, this work is based on the decomposition of input images into seven directional sub-bands and then seven sub-band images along with the input image are used as inputs to eight parallel CNNs channels. Eight probabilistic predictions originating from the input channel and seven directional sub band channels are fused for the prediction of skin lesion type.

The main novelties of this work can be summarized as follows. Primarily, a novel Gabor wavelet-based deep convolutional neural network is proposed for the detection of malignant melanoma and seborrheic keratosis. The proposed method is based on the decomposition of input images into seven directional sub-bands. Gabor based approach provides directional decomposition where each sub-band gives isolated decisions that can be fused for improved overall performance. Seven sub band images and the input image are used as inputs to eight parallel CNNs to generate eight probabilistic predictions. Decision fusion based on the sum rule is utilized to classify the skin lesion. Gabor based approach provides directional decomposition where each sub-band generates isolated directional information in the respective sub-band channel. CNN processing in each channel generates learning in the respective direction which can be regarded as decorrelated from the other directions. Hence, combining the decisions of these channels improve the overall classification performance. This approach can be regarded as an augmentation method coupled with multi-channel CNN learning.

The organization of this paper is as follows. The related work section describes previous studies on this subject. In Section 3, we describe the proposed method and give explanations for both the single and ensemble of deep convolutional neural network models. This section also explains Gabor representations and model generations. In Section 4, we report the proposed model evaluation. This section also compares the results of the proposed and other methods. Finally, we conclude the proposed methodology in Section 5.

2. Related work

There are two different classification approaches for skin lesion classification. These categories are single deep learning-based methods and the ensemble of deep learning methods.

2.1. Single deep learning based methods

Esteva et al. [1] proposed an approach for the classification of skin lesions using the GoogleNet Inception v3 deep learning model. The technique classifies three groups of skin types. First, the method detects malignant and benign types of skin lesions. Second, this technique also recognizes keratinocyte-carcinomas and seborrheic keratoses types. Finally, the study also identifies malignant melanomas and nevi. They have achieved better then dermatologists. The proposed method builds on three skin lesion datasets and then builds a model using GoogleNet Inception v3 convolutional neural network architecture. Then skin lesions are recognized using the model.

Han et al. [2] proposed Resnet-152 for the classification of skin lesions. These lesions are basal cell carcinoma, squamous cell carcinoma, intraepithelial carcinoma, actinic keratosis, seborrheic keratosis, malignant melanoma, melanocytic nevus, lentigo, pyogenic granuloma, hemangioma, dermatofibroma, and warts. This study used several datasets comprised of different ethnic groups. This study showed that ethnicity and image contrast are the factors that decrease the classification accuracy of skin lesions.

Menegola et al. [17] used six publicly available databases for skin lesion recognition. Their approach involved the training of Deep ResNet-101 and Google Inception-v4 models for malignant melanoma, seborrheic keratosis, and nevus skin lesion classification. This study showed that increasing training images by combining databases results in more accurate lesion classification.

Zhang et al. [18] proposed attention-based residual learning for melanoma, seborrheic keratosis, and nevus skin lesion classification. This method builds on the ResNet deep learning model. Attention-based layers model the last layers of this ResNet model.

Fujisawa et al. [19] proposed a four-level skin tumor detection technique. This method allows the classification of 21 skin lesion types. Skin lesion images are modeled using the GoogleLeNet, and then skin images are classified in four levels. First, malignant and benign types are recognized, and then epithelial, melanocytic categories are identified. This model also provides actinic keratosis, seborrheic keratosis, basal cell carcinoma, and Bowen disease identification.

2.2. Ensemble of the deep learning based methods

Harangi [13] proposed an ensemble of the CNN models for the classification of melanoma, seborrheic keratosis, and nevus. The proposed method fuses the output probabilities of the GoogLeNet, AlexNet, ResNet, and VGGNet models. The study also suggests four probabilistic fusion techniques for joining the models. These are the sum rule, product rule, simple majority voting, and the maximal probability rule. The sum of the maximal probabilities method leads to higher performance than other fusion techniques. This study also shows that joined models perform better than a single CNN model for skin lesion classification.

Mahbod et al. [16] proposed fusing fine-tuned deep features for skin lesion classification. This method builds on the training of several fine-tuned CNN models and then extracts features from the last fully connected layers. Then, these features are fused, and lesion classification is performed using Support Vector Machines.

Mahbod et al. [20] proposed a feature-based CNN model. The method builds on three deep convolutional neural networks. Features are extracted using AlexNet, VGG16, and ResNet-18 models. Then, the three support vector machines employ these features for skin lesion prediction.

Matsunaga et al. [21] proposed a deep neural network ensemble for the classification of melanoma, seborrheic keratosis, and nevus. Their proposed method builds on two binary classifiers. First, a classifier is generated to classify melanoma and other lesions. Second, another classifier is generated to classify seborrheic keratosis and other the skin lesions. Classifiers are created using different sets of skin lesion images and ResNet-50 models. The model fuses the output probabilities for skin lesion classification.

Nyiri and Kiss [22] proposed an ensemble of CNNs for dermatological image classification. First, the VGG16, VGG19, Xception, Inception, ResNet, and DenseNet models are generated using skin images. Then, these models are also created using segmented skin images. Then, skin image and segmented skin image-based CNN models are fused for lesion prediction. The results show that the ensemble of all models resulted in better performance than a single CNN model for lesion prediction. This study shows that ensemble CNNs outperforms each of the CNN models.

Nozdryn-Plotnicki et al. [23] generated different deep learning models, and each of these models led to the prediction of skin lesion type. The fusion of these model output probabilities provides better estimates of the skin types.

Li and Shen [24] proposed a method for the classification of melanoma, seborrheic keratosis, and nevus skin lesions. The study utilizes two ResNet models to obtain two fully connected probability maps. Then, these maps are fused for lesion type classification.

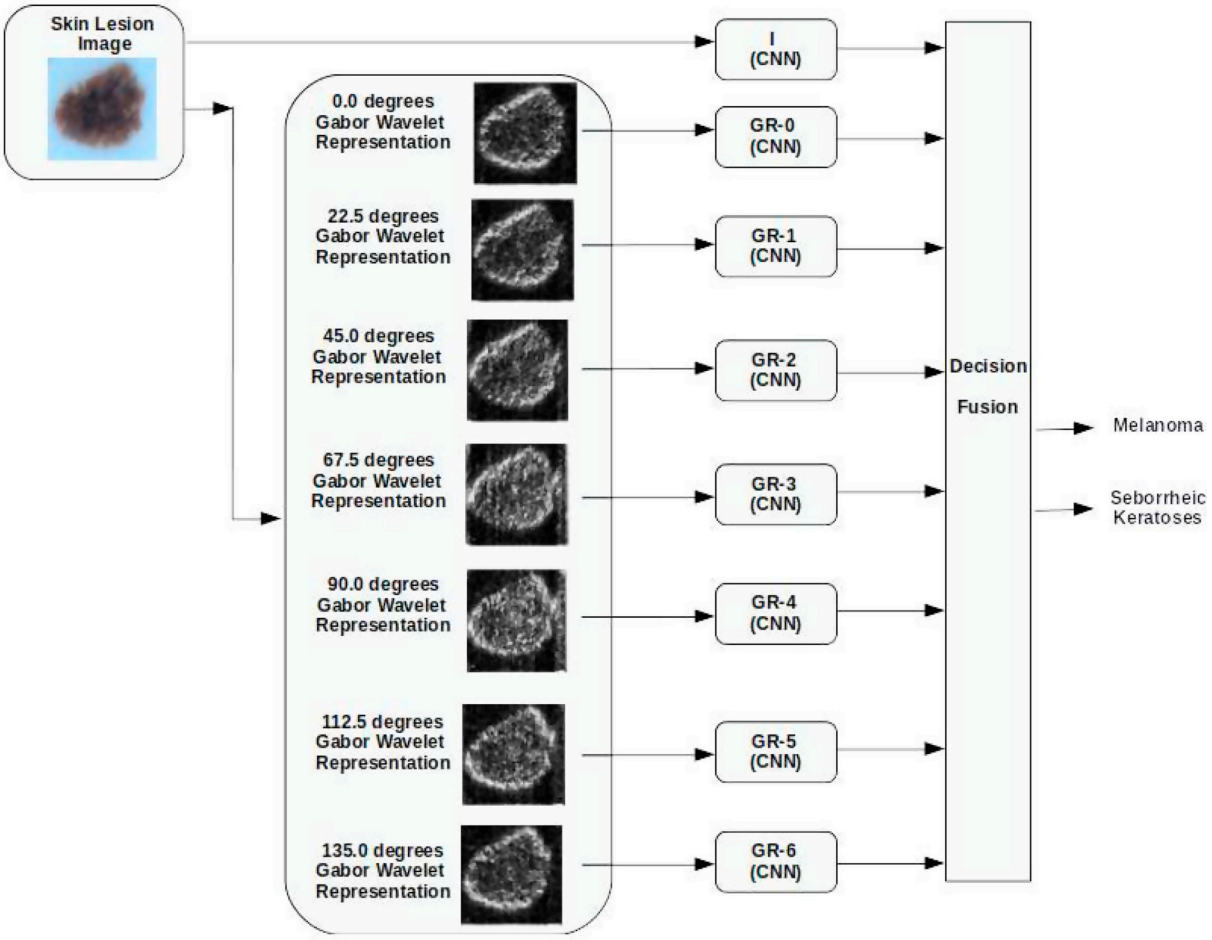

Fig. 1. The proposed gabor wavelet and image based deep convolutional neural network model for skin cancer detection.

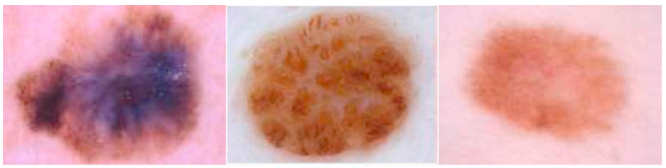

(a) Melanoma (b) Nevus (c) Nevus

Fig. 2. Skin lesion types in ISIB 2017 dataset.

Gonzalez-Diaz [25] proposed the integration of several deep learning models for the classification of melanoma, seborrheic keratosis, and nevus. These models are the lesion segmentation model, structure segmentation model, and diagnosis model. A given a skin lesion image is segmented and then used as the inputs for structure segmentation model for further feature representation. The diagnosis model uses all features to predict the final skin lesion type.

Bi et al. [26] proposed an ensemble method for skin recognition. The method allows the classification of melanoma, seborrheic keratosis, and nevus skin forms. This method builds on fusing several convolutional neural network outputs.

Recently, Hagerty et al. [27] proposed a different approach than the above studies. This approach extracts six features from skin lesion images. Then, the ResNet-50 CNN model is trained on these feature representations to obtain six feature vectors. The obtained feature vectors are mapped to skin lesion types using logistic regression.

3. Method

The proposed method builds on Gabor wavelet-based CNN models and an image-based CNN model, Fig. 1. First, seven directional Gabor wavelets represent skin images. Then, the seven Gabor-based CNN models are learned to recognize skin lesion classes. The image-based CNN model is also generated using only skin images. Finally, the CNN model outputs are combined for the estimation of melanoma and seborrheic keratosis classes (see Fig. 2).

Decision fusion allows a combination of output probabilities of CNN models. Single CNN model provides probability values for melanoma, seborrheic keratosis, and nevus skin lesions. These probabilities can be denoted by p_i where $i = 1, .., n$ and n is the number of output probabilities. In this case, the n value is equal to 3.

An ensemble of CNNs also provides output probabilities. These probabilities are denoted by p_{ij} where $i = 1, .., n$ and $j = 1,..,m$. The value of m represents the number of CNN models. This study builds on four CNN models, and the value of m equals 4.

The fusion of generated probabilities of CNN models is achieved by the sum of probabilities (SMP) [13]. The SMP is denoted by

$$p_i = \frac{\sum_{j=1}^{m} p_{ij}}{\sum_{i=1}^{n}\sum_{j=1}^{m} p_{ij}} \quad i = 1, ...n. \tag{1}$$

where p_{ij} indicates the i class probability of the CNN_j model.

3.1. Gabor wavelet representations

Fig. 3 shows skin image representation using directional Gabor

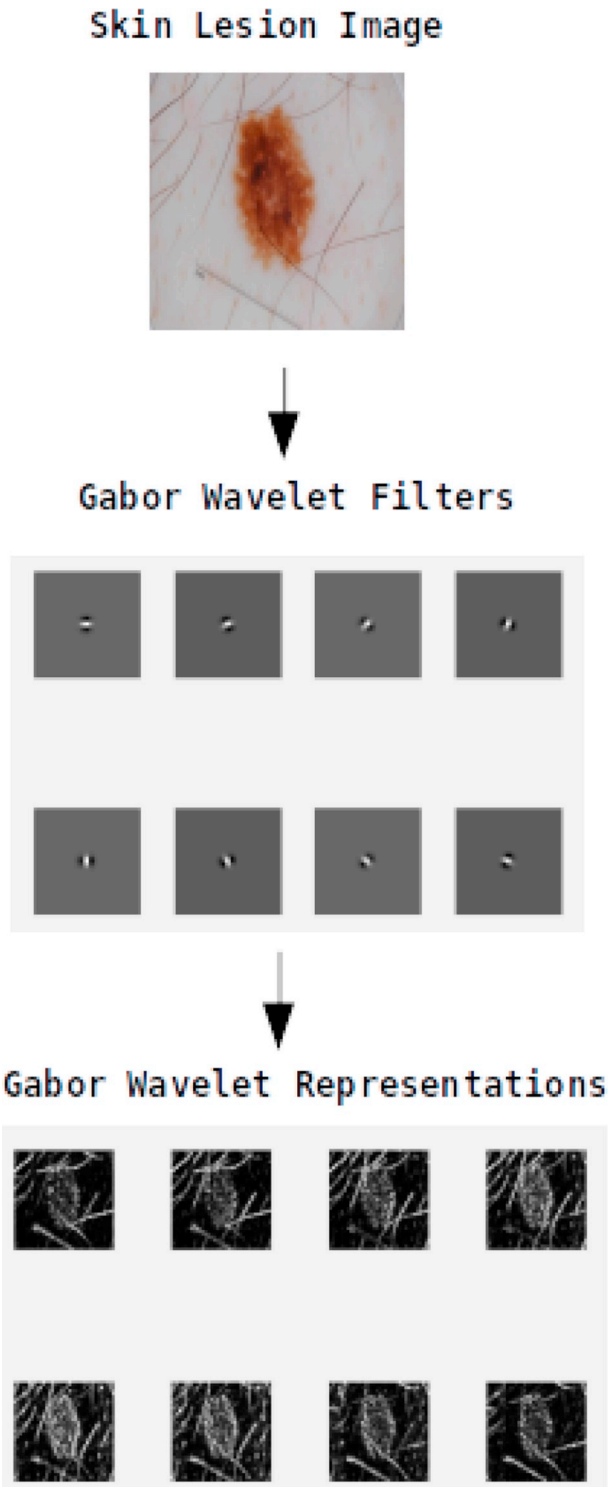

Fig. 3. Skin image representation using directional gabor wavelets.

wavelets [28]. Skin images are represented in directional detail using Gabor wavelet coefficients. Directional Gabor filters in 0°, 22.5°, 45°, 67.5°, 90°, 112.5°, 135°, 157° are applied to a skin lesion image and then corresponding directional skin image details are obtained. As a result, this approach provides orientational shape information in both spatial and frequency domains for skin images.

Gabor wavelets, 2D domain, is defined by

$$f(x,y) = e^{[x-x_0]+[y-y_0]/\alpha^2} e^{-i[u_0(x-x_0]+[v_0(y-y_0)]/\beta^2} \quad (2)$$

Table 1
ISIC 2017 dataset.

Model	Description
Melanoma	374
Seborrheic keratosis	254
Melanocytic nevus	1372
Total	2000

Table 2
The augmented dataset.

Col 1	Col 2	Col 3
Skin images	Melanoma	3366
Skin images	Seborrheic keratosis	3556
Skin images	Melanocytic nevus	4116
0° Gabor wavelet coeff.	Melanoma	3366
22.5° Gabor wavelet coeff.	Melanoma	3366
45° Gabor wavelet coeff.	Melanoma	3366
67.5° Gabor wavelet coeff.	Melanoma	3366
90° Gabor wavelet coeff.	Melanoma	3366
112.5° Gabor wavelet coeff.	Melanoma	3366
135° Gabor wavelet coeff.	Melanoma	3366
0° Gabor wavelet coeff.	seborrheic keratosis	3556
22.5° Gabor wavelet coeff.	seborrheic keratosis	3556
45° Gabor wavelet coeff.	seborrheic keratosis	3556
67.5° Gabor wavelet coeff.	seborrheic keratosis	3556
90° Gabor wavelet coeff.	seborrheic keratosis	3556
112.5° Gabor wavelet coeff.	seborrheic keratosis	3556
135° Gabor wavelet coeff.	seborrheic keratosis	3556
0° Gabor wavelet coeff.	melanocytic nevus	4116
22.5° Gabor wavelet coeff.	melanocytic nevus	4116
45° Gabor wavelet coeff.	melanocytic nevus	4116
67.5° Gabor wavelet coeff.	melanocytic nevus	4116
90° Gabor wavelet coeff.	melanocytic nevus	4116
112.5° Gabor wavelet coeff.	melanocytic nevus	4116
135° Gabor wavelet coeff.	melanocytic nevus	4116

Location is defined by (x_0, y_0) in the image and spatial frequency is denoted by $w_0 = \sqrt{u_0^2 + v_0^2}$. The orientation is also given. $\theta = arctan(v_0/u_0)$

Gabor wavelets, 2D Fourier transform, is also denoted by

$$F(u,v) = e^{\left[(u-u_0]+(v-v_0)^2\right]\alpha^2} e^{-i\left[x_0\left(u_0-v_0\right]+\left[y_0\left(v-v_0\right)\beta^2\right]} \quad (3)$$

Gabor wavelet function of the real part is located in the center of the image $x_0, y_0 = (0,0)$.

3.2. Dataset

This work uses the ISIC 2017 dataset. This dataset includes melanoma, seborrheic keratosis, and melanocytic nevus images. The number of melanoma, seborrheic keratosis, and melanocytic nevus images are 374, 254, 1372, respectively. Table 1 shows the number of skin images in the ISIC 2017 training dataset.

The Gabor wavelet filters are applied to all images of the ISIC 2017 dataset, and the corresponding Gabor wavelet coefficients of melanoma, seborrheic keratosis, and melanocytic nevus are obtained.

Then data augmentation is also carried out for skin images and Gabor representations. The melanoma and seborrheic keratosis images are rotated 18° while melanocytic nevus is rotated 45° degrees. The skin images and corresponding Gabor wavelets can be seen in Table 2.

Table 3
Generated models for skin images and gabor wavelet coefficients.

Model	Description
I	CNN for Skin images
G0	CNN for $\mathbf{0}^{\circ}$ Gabor Wavelet Coeff.
G1	CNN for $\mathbf{22.5}^{\circ}$ Gabor Wavelet Coeff.
G2	CNN for $\mathbf{45}^{\circ}$ Gabor Wavelet Coeff.
G3	CNN for $\mathbf{67.5}^{\circ}$ Gabor Wavelet Coeff.
G4	CNN for $\mathbf{90}^{\circ}$ Gabor Wavelet Coeff.
G5	CNN for $\mathbf{112.5}^{\circ}$ Gabor Wavelet Coeff.
G6	CNN for $\mathbf{135}^{\circ}$ Gabor Wavelet Coeff.
GR	CNN for Seven gabor Wavelet Coeff.
I-GR	CNN for Image and Seven Gabor Wavelet Coeff.
I-GR0235	CNN for $\mathbf{0}^{\circ}, \mathbf{45}^{\circ}, \mathbf{67.5}^{\circ}, \mathbf{112.5}^{\circ}$ Gabor Wavelet Coeff.

3.3. Gabor CNN model generations

Table 3 shows the generated models for the proposed Gabor based CNN model. I represents the generated CNN model for skin image data. The other seven Gabor based CNN models are G0, G1, G2, G3, G4, G5, G6, G6, and G7. G0 is the CNN model, and it is trained using 0° Gabor wavelet representations of the skin images. Similarly, G1, G2, G3, G4, G5, G6, G6, and G7 are the CNN models, and they are generated using 22.5°, 45°, 67.5°, 90°, 112.5°, 135°, 157° Gabor representations respectively.

GR model describes the fused Gabor wavelet-based CNN model. This model is developed by training seven CNN models for seven Gabor wavelet representations and then fusing the output probabilities. Section 3 explains the fusing process. Similarly, the I-GR model describes the unified image and Gabor wavelet-based CNN model. This model is created by training seven CNN models for seven Gabor wavelet representations and a CNN model for skin images. Then, the output probabilities are combined for skin type classification.

Wavelet and skin image-based CNN models build on the AlexNet, and ResNet-18 models. These CNN models are the pretraned ImageNet [29]. The proposed method uses these trained AlexNet and ResNet-18 models to fine-tune them for the skin lesion types. Pre-trained models allow better estimation of network parameters together with ISIC 2017 images.

4. Performance evaluation

The performance of the proposed Gabor wavelet-based deep learning model is evaluated for melanoma and seborrheic keratosis recognition tasks. The area under the receiver operating characteristic curve (M-AUC), accuracy (M-ACC), sensitivity (M-SE), and specificity (M-SP) shows the performance of the melanoma. Similarly, the area under the receiver operating characteristic curve (SK-AUC), accuracy (SK-ACC), sensitivity (SK-SE), and specificity (SK-SP) defines the performance of seborrheic keratosis. The average area under the receiver operating characteristic curve (AVG-AUC) is also defined for melanoma and seborrheic keratosis lesion types. The performance evaluation of the proposed methods is evaluated using the publicly available ISIC 2017 dataset. This dataset contains skin lesion images of melanoma, seborrheic keratosis, and nevus classes.

Table 4
The performances of the proposed models.

CNN for Image	CNN for Gabor	Method	AVG-AUC	M-AUC	M-ACC	M-SE	M-SP	SK-AUC	SK-ACC	SK-SE	SK-SP
AlexNet	–	**I**	**0.72**	**0.86**	0.81	0.23	0.95	**0.58**	0.81	0.62	0.88
ResNet-18	–	**I**	**0.69**	**0.77**	**0.83**	0.30	0.96	**0.61**	0.82	0.74	0.85
-	AlexNet	**GR-0**	**0.78**	**0.84**	0.77	0.10	0.93	**0.71**	0.56	0.17	0.71
-	AlexNet	**GR-1**	**0.80**	**0.82**	0.79	0.13	0.95	**0.77**	0.68	0.10	0.91
-	AlexNet	**GR-2**	**0.82**	**0.83**	0.78	0.37	0.88	**0.80**	0.71	0.17	0.92
-	AlexNet	**GR-3**	**0.86**	**0.91**	0.82	0.30	0.95	**0.80**	0.71	0.17	0.92
-	AlexNet	**GR-4**	**0.83**	**0.82**	0.81	0.30	0.93	**0.84**	0.73	0.38	0.87
-	AlexNet	**GR-5**	**0.86**	**0.86**	0.80	0.20	0.95	**0.85**	0.71	0.17	0.92
-	AlexNet	**GR-6**	**0.60**	**0.80**	0.71	0.10	0.87	**0.40**	0.45	0.57	0.40
-	AlexNet	**GR**	**0.78**	**0.85**	0.79	0.17	0.95	**0.70**	0.71	0.48	0.80
AlexNet	AlexNet	**I-GR**	**0.88**	**0.95**	0.82	0.20	0.98	**0.80**	0.65	0.33	0.78
ResNet-18	AlexNet	**I-GR**	**0.79**	**0.84**	0.79	0.17	0.95	**0.73**	0.69	0.50	0.77
ResNet-18	AlexNet	**I-GR0235**	**0.91**	**0.96**	0.83	0.13	1.00	**0.86**	0.82	0.17	0.98

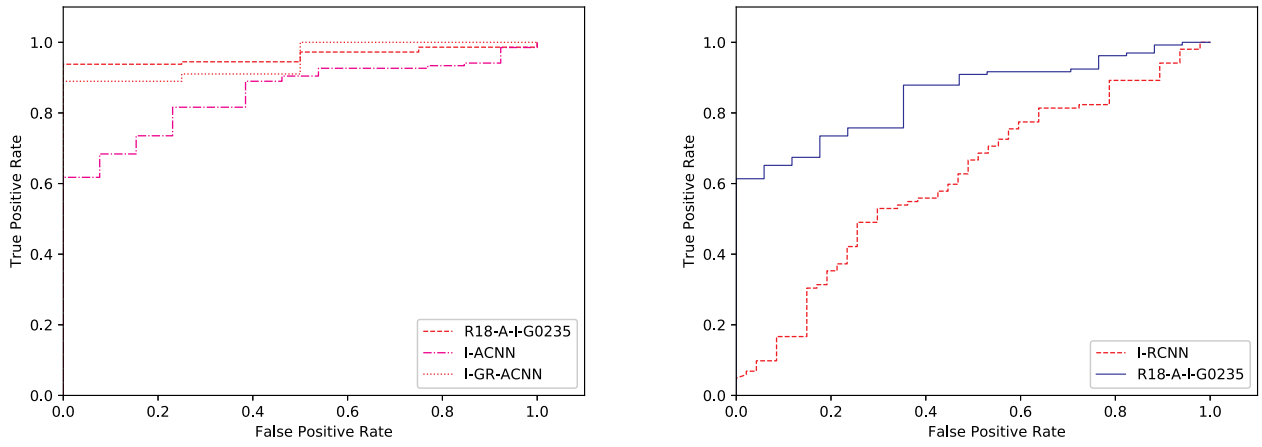

(a) Melanoma (b) Seborrheic Keratosis

Fig. 4. The performance comparions of melanoma and seborrheic keratosis.

Table 5
The performance comparision of the proposed models.

Network	Method	AVG-AUC	M-AUC	M-ACC	M-SE	M-SP	SK-AUC	SK-ACC	SK-SE	SK-SP
GR	**Gabor based CNN**	**0.78**	**0.85**	0.79	0.17	0.95	**0.70**	0.71	0.48	0.80
I-GR	**Gabor and AlexNet**	**0.88**	**0.95**	0.82	0.20	0.98	**0.80**	0.65	0.33	0.78
I-GR	**Gabor and ResNet-18**	**0.79**	**0.84**	0.79	0.17	0.95	**0.73**	0.69	0.50	0.77
I-GR0235	**Gabor and ResNet-18**	**0.91**	**0.96**	0.83	0.13	1.00	**0.86**	0.82	0.17	0.98
Haragi [13]	Ensembles of CNNs	0.89	0.85	0.85	0.40	0.71	0.93	0.88	0.71	0.85
Zhang et al. [18].	Attention based CNN	0.90	0.86	0.84	0.59	0.89	0.95	0.90	0.87	0.93
Li and Shen [24]	Lesion Indexing	–	0.91	0.86	0.49	0.96	–	–	–	–
Matsunaga et al. [21].	Ensembles of CNNs	0.91	0.87	0.83	0.73	0.85	0.95	0.80	0.98	0.77
Diaz [25]	Knowledgebased CNN	0.91	0.85	0.82	0.10	0.99	0.96	0.87	0.17	0.99
Menegola et al. [17].	Ensembles of CNNs	0.91	0.87	0.87	0.54	0.95	0.94	0.89	0.35	0.99
Bi et al. [26].	Ensembles of CNNs	0.89	0.87	0.85	0.42	0.96	0.92	0.91	0.58	0.97
Mahbod et al. [16].	Deep features	0.91	0.87	–	–	–	0.95	–	–	–
Mahbod et al. [20].	Hybird CNNs	0.90	0.84	–	–	–	0.97	–	–	–
Hagerty et al. [27].	HC Ensemble	–	0.90	–	–	–	–	–	–	–
Hagerty et al. [27].	HC and DL Ensemble	–	0.94	–	–	–	–	–	–	–

4.1. Gabor wavelet based method

Table 4 shows all generated model performances. The best performing model is I-GR0235 among the other models. This model provides a value of 0.96% M-AUC melanoma classification. This model also gives a value of 86.0% for SK-AUC. The AVG-AUC is 91.0%. Additionally, the GR model results in values of $0.78, 0.85, 0.70\%$ for AVG-AUC, M-AUC, and SK-AUC, respectively. Moreover, the I-GR models lead to values of $0.88, 0.95, 0.80\%$ for AVG-AUC, M-AUC, and SK-AUC, respectively. As a result, the image and Gabor-based CNN provided higher recognition value when they were combined for skin type prediction.

Fig. 4 shows the receiver operating characteristic curves for melanoma and seborrheic keratosis. First, Fig. 4 (a) gives comparisons of the R18-A-I-G0235, I-ACNN, and I-GR-ACNN models. The best performing model is R18-A-I-G0235. This model outperforms the only image-based I-ACNN model. R18-A-I-G0235 builds on the image-based ResNet-18, and the seven Gabor wavelet-based AlexNet model. Finally, Fig. 4 (b) presents a comparison of I-RCNN and R18-A-I-G0235 models. R18-A-I-G0235 also outperforms the I-RCNN model.

4.2. Comparison of the proposed methods

Table 5 shows a comparison between the proposed Gabor wavelet-based CNN model and other recently developed CNN methods. The proposed I-GR and I-GR0235 models outperform all other proposed methods for melanoma detection. The M-AUC values of these models are 0.95.0% and 96.0% respectively. The proposed I-GR0235 model provides 0.91.0%, 96.0% and 0.86% for AVG-AUC, M-AUC, SK-AUC respectively.

5. Conclusion

This work proposes a novel Gabor wavelet-based deep learning model for melanoma and seborrheic keratosis. This model builds on an ensemble of seven Gabor wavelet-based CNN models. Furthermore, this model fuses the Gabor wavelet-based model and an image-based CNN model. The performance evaluation results show that an ensemble of the image and Gabor wavelet-based model outperforms a single image and Gabor wavelet-based models. This ensemble also outperformed the group of only Gabor wavelet-based CNN models. The proposed unified CNN model generates more effective skin type classification than the other proposed methods.

References

[1] L.R. Siegel, K.D. Miller, A. Jemal, Cancer statistics, Cancer J. 547 (68) (2018) 7–30.

[2] A. Esteva, B. Kuprel, A.,R. Novoa, M.,S. Swetter, M.H. Blau, S. Thrun, Dermatologist-level classification of skin cancer with deep neural networks, Nature 547 (2) (2017) 115–118.

[3] S.,S. Han, M.,S. Kim, W. Lim, G.,H. Park, I. Park, S.E. Chang, Classification of the clinical images for benign and malignant cutaneous tumors using a deep learning algorithm, J. Investig. Dermatol. 138 (2018).

[4] P. Tschandl, C. Rosendahl, H. Kittler, The HAM10000 Dataset: A Large Collection of Multi-Source Dermatoscopic Images of Common Pigmented Skin Lesions, 2018. ArXiv.

[5] K.,S. Nehal, C.,K. Bichakjian, Update on keratinocyte carcinomas, N. Engl. J. Med. 379 (4) (2018) 363–374.

[6] R.,B. Oliveira, João P. Papa, A. Pereira, S. Tavares, R.S. João Manuel, Computational Methods for Pigmented Skin Lesion Classification in Images: Review and Future Trends, vol. 29, 2015, pp. 613–636 (3).

[7] A.C. Geller, B.A. Dickerman, J.M. Taber, L.A. Dwyer, A.M. Hartman, F.M. Perna, Skin Cancer Interventions across the Cancer Control Continuum: A Review of Experimental Evidence (1/1/2000–6/30/2015) and Future Research Directions, vol. 111, 2018, pp. 442–450.

[8] Y. Li, L. Shen, Dermoscopy image analysis: overview and future directions, IEEE J. Biomed. Health Inf. 23 (2) (2019) 474–478.

[9] C. Szegedy, W. Liu, Y. Jia, P. Sermanet, S. Reed, D. Anguelov, D. Erhan, V. Vanhoucke, A. Rabinovich, Going deeper with convolutions, in: IEEE Conference on Computer Vision and Pattern, 2015.

[10] C. Szegedy, V. Vanhoucke, S. Ioffe, J. Shlens, Z. Wojna, Rethinking the inception architecture for computer vision, in: IEEE Conference on Computer Vision and Pattern Recognition, 2016.

[11] S. Targ, D. Almeida, K. Lyman, Resnet in Resnet: Generalizing Residual Architectures, CoRR, 2016.

[12] S. Kaymak, A. Serener, Deep learning for two-step classification of malignant pigmented skin lesions, in: Symposium on Neural Networks and Applications, 2018.

[13] B. Harangi, Skin lesion classification with ensembles of deep convolutional neural networks, Biomed. Inf. 86 (2018) 25–32.

[14] A. Krizhevsky, I. Sutskever, G.,E. Hinton, Imagenet classification with deep convolutional neural networks, in: Proceedings of the 25th International Conference on Neural Information Processing Systems, vol. 1, Curran Associates Inc, USA, 2012, pp. 1097–1105. NIPS'12.

[15] K. Simonyan, A. Zisserman, Very deep convolutional networks for large-scale image recognition, in: International Conference on Learning Representations, 2015.

[16] A. Mahbod, G. Schaefer, I. Ellinger, R. Ecker, A. Pitiot, C. Wang, Fusing fine-tuned deep features for skin lesion classification, Comput. Med. Imag. Graph. 71 (2019) 19–29.

[17] A. Menegola, J. Tavares, M. Fornaciali, L.T. Li, S. Avila, E. Valle, RECOD titans at ISIC challenge 2017 (Online). Available: https://arxiv.org/pdf/1703.04819.

[18] J. Zhang, Y. Xie, Y. Xia, C. Shen, Attention Residual Learning for Skin Lesion Classificatio, 2019.

[19] Y. Fujisawa, Y. Otomo, Y. Ogata, Y. Nakamura, R. Fujita, Y. Ishitsuka, R. Watanabe, N. Okiyama, K. Ohara, M. Fujimoto, Deep-learning-based, computer-aided classifier developed with a small dataset of clinical images surpasses board-certified dermatologists in skin tumour diagnosis, Br. J. Dermatol. 180 (2019) 373–381.

[20] A. Mahbod, G. Schaefer, C. Wang, R. Ecker, I. Ellinger, Skin Lesion Classification Using Hybird Deep Neural Networks, ICASSP, 2019.

[21] K. Matsunaga, A. Hamada, A. Minagawa, H. Koga, Image Classification of Melanoma, Nevus and Seborrheic Keratosis by Deep Neural Network Ensemble, 2017. ArXiv.

[22] T. Nyiri, A. Kiss, Novel ensembling methods for dermatological image classification, in: Int. Conf. Theory and Practice of Natural Computing, 2018.

[23] A. Nozdryn-Plotnicki, J. Yap, W. Yolland, Ensembling Convolutional Neural Networks for Skin Cancer Classification, 2018. ArXiv.

[24] Y. Li, L. Shen, Skin Lesion Analysis towards Melanoma Detection Using Deep Learning Network, vol. 18, 2018, p. 556 (2).

[25] I.G. Gonzalez-Diaz, Incorporating the Knowledge of Dermatologists to Convolutional Neural Networks for the Diagnosis of Skin Lesions, 2017.
[26] L. Bi, J. Kim, E. Ahn, D. Feng, Automatic Skin Lesion Analysis Using Large-Scale Dermoscopy Images and Deep Residual Networks, 2018.
[27] J. Hagerty, R. Stanley, H. Almubarak, N. Lama, R. Kasmi, P. Guo, R. Drugge, H. Rabinovitz, M. Olivero, W. Stoecker, Deep Learning and Handcrafted Method Fusion: Higher Diagnostic Accuracy for Melanoma Dermoscopy Images, 2019.
[28] Computer Science Tripos, Part II: 16 Lectures.
[29] J. Deng, W. Dong, R. Socher, L.,J. Li, K. Li, L. Fei-Fei, ImageNet: a large-scale hierarchical image database, in: IEEE Computer Vision and Pattern Recognition, 2009.